Cent. Eur. J. Phys. • 7(2) • 2009 • 227-231
DOI: 10.2478/s11534-009-0025-9

VERSITA

Central European Journal of **Physics**

Passivation of defect states in surface and edge regions on pn-junction Si solar cells by use of hydrogen cyanide solutions

Research Article

Masao Takahashi*, Takeru Shishido, Hitoo Iwasa, Hikaru Kobayashi

ISIR, Osaka University and CREST, Japan Science and Technology Agency, 8-1, Mihogaoka, Ibaraki, Osaka 567-0047, Japan

Received 6 December 2008; accepted 9 March 2009

Abstract: The local photovoltage of the pn-junction single-crystalline silicon solar cells observed by spot light scanning gradually decreases in the vicinity of edges. The energy conversion efficiency is increased by shadowing the edge regions where the local photovoltage is lower, showing that the defect density is high in the edge regions. From the analysis of the local photovoltage, the spacial distribution of defect states is obtained. The cyanide method, *i.e.*, immersion of solar cells in HCN solutions at room temperature, increases the local photovoltage and increases the energy conversion efficiency.

PACS (2008): 68.35.bg; 72.40.+w; 81.65.Rv; 89.30.Cc

Keywords: defect passivation • cyanide method • silicon solar cell • local photovoltage • energy conversion efficiency

1. Introduction

Defect states such as Si dangling bonds seriously degrade performance of Si solar cells even when their concentration is very low. Several defect passivation methods applicable to Si materials have been developed, e.g., hydrogen plasma treatment [1, 2], forming gas annealing [3, 4], deposition of a hydrogen-containing silicon nitride layer [4, 5], wet-chemical passivation [6], *etc.* We have also developed a method of defect passivation for semiconductor devices called cyanide method [7–13] which can simultaneously remove metal contaminants [14–19]. The cyanide method simply includes immersion of Si materials in dilute cyanide solutions such as HCN aqueous solutions at room temperature. Si-CN bonds formed from Si dangling bonds by the cyanide method are stable at high temperatures (e.g., 800°C) and under irradiation of visible and UV lights, resulting in thermal and irradiation stability of the cyanide method [9].

In the present study, a simple method, *i.e.*, measurements of a photovoltage generated by irradiation with a monochromatic laser spot, has been used to elucidate the distribution of defect states. The defect states present in the surface region and the edge region are passivated by the cyanide method.

*E-mail: m.takahashi@sanken.osaka-u.ac.jp

Table 1. Open circuit photovoltage, V_{OC}, short-circuit photocurrent density, J_{SC}, fill factor, FF, and energy conversion efficiency, η, for pn- junction c-Si solar cells with and without passivation by the cyanide method.

	V_{OC} (V)	J_{SC} (mA/cm^2)	FF	η (%)
without passivation	0.548	33.1	0.615	11.2
with passivation	0.550	33.4	0.661	12.2
improvement	0.365%	0.906%	7.48%	8.93%

2. Experiment

pn-junction single crystalline Si (c-Si) wafers with mat-textured structure were cut into 25.4 × 25.4 mm^2 pieces and cleaned using the RCA method [20]. ∼1 μm thick-aluminum (Al) electrodes were formed on the rear Si surface using the vacuum evaporation method. Then, front silver (Ag) electrodes were formed by screen-printing Ag paste, followed by drying at 150°C and heating at 690°C in the mixed gas of oxygen and nitrogen. For the heat treatment, oxygen and nitrogen flow rates were set at 0.1 and 0.9 dm^3/min, respectively.

The cyanide method was performed by immersion of the Si specimens in a 0.1 M HCN aqueous solution with pH in the range between 9 and 10 for 3 min at room temperature, followed by rinse in ultra-pure water. pH of the solutions was regulated by addition of tetramethyl ammonium hydroxide solutions.

For some specimens, the edge region was etched locally with 30wt% KOH aqueous solutions (KOH treatment), followed by heating at 90°C for 30 s [21].

Photocurrent-photovoltage ($I_{ph} - V_{ph}$) curves were measured under AM 1.5 100 mW/cm^2 irradiation using a DC voltage/current source. The local photovoltage measurements were performed under irradiation by a 5 mW laser diode with the wavelength of 655 nm. The laser beam was focused on the sample surface by a pin-hole and condensing lenses; the beam size on the sample surface was 0.3 mm in diameter. Position-dependence of the photovoltage was measured by moving a sample stage every 0.03 mm in the vertical direction with respect to the laser beam.

3. Results

Fig. 1 shows $I_{ph} - V_{ph}$ curves of the pn-junction c-Si solar cell with and without passivation by the cyanide method. The solar cell characteristics are summarized in Tab. 1. With passivation, the fill factor and the energy conversion efficiency were increased by 7.48 and 8.93%, respectively.

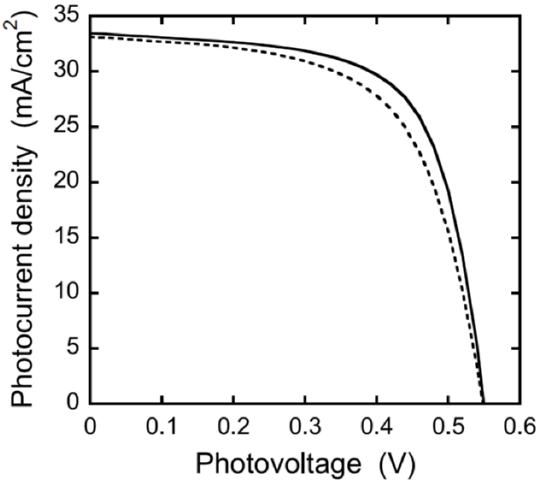

Figure 1. Photocurrent-photovoltage curves for pn-junction single crystalline Si solar cells: Solid and dashed lines are for the solar cells with and without passivation, respectively by the cyanide method.

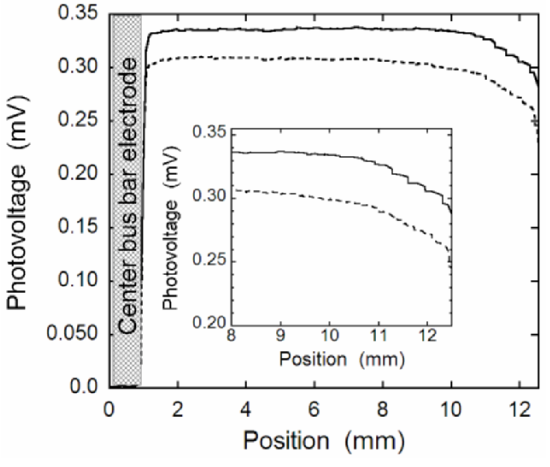

Figure 2. Position-dependency of the photovoltage for the same solar cells as Fig. 1: Solid and dashed lines are for the solar cells with and without passivation, respectively, by the cyanide method. The inset shows the enlarged plots near the edge region.

Fig. 2 shows the local photovoltage measured from a center bus bar electrode to a cell edge for the solar cell with and without passivation by the cyanide method. The photovoltage was nearly constant up to 11 mm from the center electrode, and gradually decreased in the vicinity of the edge (*i.e.*, in the region less than 2 mm from the edge). The photovoltage was increased by the passivation, especially the increase in the edge region being noticeable. The decrease in the photovoltage near the edge region is attributable to defect states, as described later.

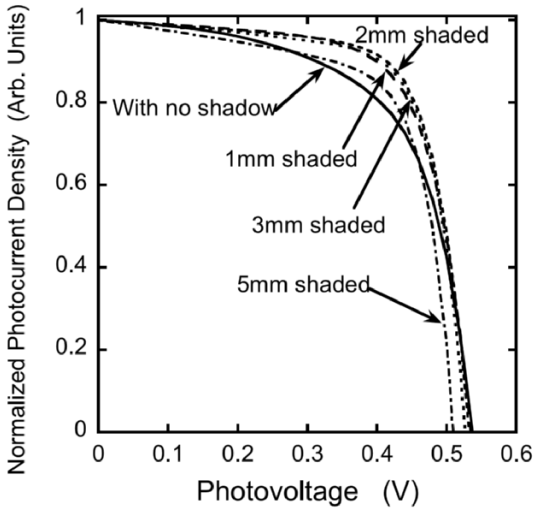

Figure 3. Photocurrent-photovoltage curves for the solar cells whose edge parts are shadowed.

Table 2. The fill factor, FF, and energy conversion efficiency, η for pn-junction single crystalline Si solar cells with shading edge regions.

Width covering edges (mm)	FF	η (%)
0	0.605	10.9
1	0.681	13.8
2	0.703	14.2
3	0.702	13.7
5	0.673	13.6

Fig. 3 shows $I_{ph} - V_{ph}$ curves of the pn-junction Si solar cells in which the edge regions were shadowed in order to avoid generation of electron-hole pairs there. When the shadow area was 2 mm or less from each edge, both the fill factor and the energy conversion efficiency increased with increasing the shadow area, as listed in Tab. 2. With more shadowing, both the fill factor and the energy conversion efficiency decreased.

The solar cell characteristics were measured before and after etching off the edge region by the KOH treatment (30wt% KOH aqueous solutions at 90°C for 30 s) (Tab. 3). After etching off the edge region by 0.1 mm, the fill factor and the energy conversion efficiency were increased by 3.31 and 3.67%, respectively.

Table 3. Open circuit photovoltage, V_{OC}, short-circuit photocurrent density, J_{SC}, fill factor, FF, and energy conversion efficiency, η, for pn- junction single crystalline Si solar cells before and after etching off the edge region by the KOH treatment.

	V_{OC} (V)	J_{SC} (mA/cm^2)	FF	η (%)
before etching	0.537±0.004	33.6±0.8	0.604±0.004	10.9±0.4
after etching	0.539±0.003	33.7±0.4	0.624±0.02	11.3±0.6

4. Discussion

Under illumination, the current density, J, can be expressed as a sum of a photocurrent density, J_{ph}, and a dark current density, J_{dark} [22],

$$J = J_{ph} + J_{dark}, \tag{1}$$

in which J_{dark} is given by the sum of several current components:

$$J_{dark} = \sum_i J_i^0 \left[\exp\left(\frac{qV}{n_i kT} \right) - 1 \right], \tag{2}$$

where J_i^0 and n_i are the dark saturation current density, and the ideality factor, respectively, for the i-th component and V is the photovoltage. It is likely that the dark current in the non-edge region is composed of only the minority carrier diffusion current which possesses an ideality factor of unity;

$$J_{dark} = J_{\min}^0 \exp\left(\frac{qV}{kT} \right), \tag{3}$$

where $J_{\min}^0$ is the minority carrier diffusion dark saturation current density. The local photovoltage in the edge region is lower than that in the non-edge region, which is likely to be due to the recombination current in addition to the diffusion current:

$$J_{dark}(x) = J_{\min}^0 \exp\left(\frac{qV(x)}{kt} \right) + J_{rec}^0 \exp\left(\frac{qV(x)}{2kT} \right), \tag{4}$$

where x denotes the position in the edge region. For the recombination current, 2 is the most probable value for the ideality factor, n [22]. Since the local photovoltage was measured at the identical photocurrent density for both the edge and non-edge regions, we have

$$J_{\min}^0 \exp\left(\frac{qV_n}{kt} \right) = J_{\min}^0 \exp\left(\frac{qV(x)}{kt} \right) + J_{rec}^0 \exp\left(\frac{qV(x)}{2kT} \right), \tag{5}$$

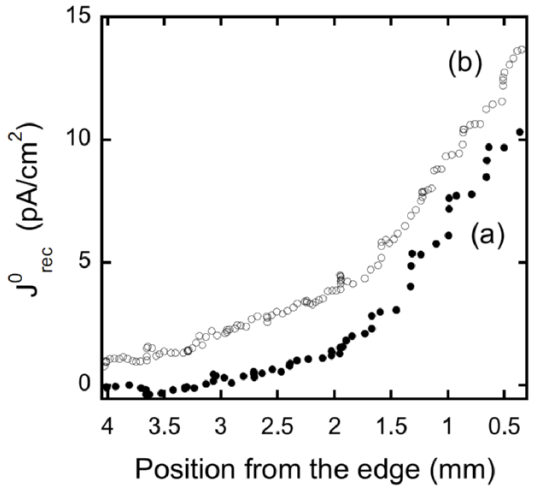

Figure 4. Plots of the recombination current density *vs.* the distance from the cell edge: (a) With and (b) without the passivation, respectively.

where V_n is the local photovoltage in the non-edge region. From Eq. (5), J^0_{rec} is expressed by

$$J^0_{rec} = J^0_{\min} \exp\left(-\frac{qV(x)}{2kT}\right) \left[\exp\left(\frac{qV_n}{kT}\right) - \exp\left(\frac{qV(x)}{kT}\right)\right]. \quad (6)$$

Fig. 4 shows J^0_{rec} which is calculated using Eq. (6) and 8.19 μA/cm^2 for $J^0_{\min}$ obtained from the y-axis intercept of the semi-log plot of the dark current density *vs.* voltage in the reverse bias region. The plot clearly shows that J^0_{rec} increases in the edge-region. It should be noted that the recombination current density is proportional to the density of defect states, and thus, the defect density possesses the same spacial distribution. With the defect passivation by the cyanide method, the increase in J^0_{rec} is suppressed in the edge region, indicating that the cyanide method can passivate defect states there.

When the shadowing distance from the edge is less than 2 mm, the energy conversion efficiency increases (*cf.* Fig. 3 and Tab. 2). The length of 2 mm is in accordance with the region where the local photovoltage decreases (Fig. 2). Therefore, it can be concluded that the shadowing avoids photo-generation of electrons and holes in the defective region in which they easily recombine. With a further increase in the shadowing area, the energy conversion efficiency decreases, mainly due to a decrease in the open-circuit photovoltage, V_{OC}. V_{OC} is expressed by a ratio between J_{ph} and J^0_{dark}:

$$V_{OC} = \frac{nkT}{q} \ln\left(\frac{J_{ph}}{J^0_{dark}} + 1\right). \quad (7)$$

An increase in the shadowed area decreases J_{ph} while J^0_{dark} is not affected by the shadowing. Therefore, the shadowing of non-defective area decreases J_{ph}/J^0_{dark}, leading to a decrease in V_{OC}.

It is expected that removal of edge regions with high density defects improves solar cell characteristics. However, as listed in Tab. 3, the cell characteristics cannot be improved effectively by removing only the edge regions (removal area: 9.2 mm^2) using the KOH treatment. On the other hand, the defect passivation by the cyanide method performed on the whole cell surface can improve the cell characteristics more effectively because defect states present in the edge region and the surface region are both eliminated (*cf.* Tab. 1).

5. Conclusion

The spacial distribution of the defect state density in the solar cells has been obtained by measurements of the local photovoltage generated by the laser beam, and the following results and conclusions are obtained.

(1) The density of defect states increases towards the edges of the solar cells.

(2) The cyanide method, *i.e.*, immersion of solar cells in HCN aqueous solutions, can passivate defect states and consequently increases the local photovoltage, leading to increases in the fill-factor and the energy conversion efficiency.

References

[1] J. V. Rao, W. A. Anderson, G. Rajeswaram, Phys. Status Solidi A 72, 745 (1982)
[2] J. L. Hanoka, C. H. Seager, D. J. Sharp, J. K. G. Panitz, Appl. Phys. Lett. 42, 618 (1983)
[3] P. Sana, A. Rohatgi, J. P. Kalejs, R. O. Bell, Appl. Phys. Lett. 64, 97 (1994)
[4] R. Koshore, H. R. Moutinho, B. L. Sopori, Renew. Energ. 6, 589 (1995)
[5] F. Duerinckx, J. Szlufcik, Sol. Ener. Mat. Sol. C. 72, 231 (2002)
[6] H. Angermann, W. Henrion, M. Rebien, A. Roseler, Sol. Ener. Mat. Sol. C. 83, 331 (2004)
[7] H. Kobayashi et al., J. Appl. Phys. 83, 2098 (1998)
[8] T. Kubota et al., Surf. Sci. 529, 329 (2003)

[9] O. Maida, A. Asano, M. Takahashi, H. Iwasa, H. Kobayashi, Surf. Sci. 542, 244 (2003)
[10] H. Kobayashi, S. Tachibana, K. Ymanaka, Y. Nakato, K. Yoneda, J. Appl. Phys. 81, 7630 (1997)
[11] H. Kobayashi, S. Tachibana, Y. Nakato, K. Yoneda, J. Electrochem. Soc. 144, 2893 (1997)
[12] E. Kanazaki, K. Yoneda, Y. Todokoro, M. Nishitani, H. Kobayashi, Solid State Commun. 113, 195 (2000)
[13] H. Kobayashi, Y. Kasama, T. Fujinaga, M. Takahashi, H. Koinuma, Solid State Commun. 123, 151 (2002)
[14] N. Fujiwara et al., Appl. Surf. Sci. 235, 372 (2004)
[15] M. Takahashi, Y.-L. Liu, N. Fujiwara, H. Iwasa, H. Kobayashi, Solid State Commun. 137, 263 (2006)
[16] Y.-L. Liu et al., Surf. Sci. 600, 1165 (2006)
[17] N. Fujiwara, Y.-L. Liu, M. Takahashi, H. Kobayashi, J. Electrochem. Soc. 153, G394 (2006)
[18] Y.-L. Liu, M. Takahashi, H. Kobayashi, J. Electrochem. Soc. 154, H16 (2007)
[19] H. Narita, M. Takahashi, H. Iwasa, H. Kobayashi, J. Electrochem. Soc. 155, H103 (2008)
[20] W. Kern, D. Puotinen, RCA Rev. 31, 187 (1970)
[21] M. H. Al-Rifai, J. Carstensen, H. Foll, Sol. Ener. Mat. Sol. C. 72, 327 (2002)
[22] S. M. Sze, Physics of Semiconductor Devices, 2nd edition (Wiley, New York, 1981)